

The mechanical behaviour of PEEK short fibre composites

J. R. SARASUA*, P. M. REMIRO

Polimeroen Zientzia eta Teknologia Saila, Kimika Fakultatea, Euskal Herriko Unibertsitatea, P.O. Box 1072, 20080 Donostia, Spain

J. POUYET

Laboratoire de Mécanique Physique, CNRS URA n° 867, Université de Bordeaux I, 33405 Talence, France

Short glass (GF) and carbon fibre (CF) reinforced poly-ether-ether-ketone (PEEK) composites were prepared by injection moulding and then microstructurally characterized. Their mechanical behaviour was determined by two different methods: a classical unidirectional tensile test and an immersion ultrasonic technique. The reinforcing effect of fibres is discussed in the context of the theory of reinforcement of Bowyer and Bader. Interfacial shear strength and critical fibre length at break are calculated for both PEEK/GF and PEEK/CF composites. Examinations of fracture surfaces of uniaxial tensile specimens revealed a higher adhesion of carbon fibres to PEEK matrix in regards to the adhesion concerning glass fibre–PEEK interfaces, which is in agreement with the results provided by the model. Compatibility of ultrasonic and tensile results is reported.

1. Introduction

Short fibre reinforced thermoplastics (SFRTTP) are intermediate materials between unreinforced polymers and classical long fibre composites. Comparing the properties of SFRTTP with those of unreinforced polymers is commonly observed that the incorporation of chopped fibres in a thermoplastic matrix produces significant improvements in stiffness and strength, though there is often a marked reduction in ductility. Since SFRTTP consist of chopped and often disoriented fibres, they cannot compete in stiffness and strength with the classical unidirectional long fibre composites. This disadvantage, however, is compensated by the fact that they can be manufactured by usual processing methods for thermoplastics such as extrusion and injection moulding permitting them to be suitable to cover a wide field of practical applications: electrical connectors, hot water meters, automobile engine components, aircraft parts or valve components, where they are replacing metals [1].

The basic approach to predict the strength of short fibre composites began with the work of Cox [2] in 1952, which served as the basis for the ulterior development of the critical fibre concept used by Kelly and Tyson to describe the mechanical behaviour of short fibre reinforced metals [3]. As SFRTTP are concerned, Bowyer and Bader developed an expression in which the strength of commercial SFRTTP could be predicted

taking into account the contribution to the composite strength of subcritical and supercritical fibres, and that of the matrix [4].

The problem to predict the stress–strain behaviour of SFRTTP is particularly complex since their microstructure is closely related to the thermomechanical history carried out during the manufacturing process. In fact, the state of orientation of fibres and final fibre length values, as well as matrix ability to crystallize are dependent on processing conditions that will vary in function of the polymeric material chosen for the matrix.

The application of the above mentioned model for SFRTTP has been limited to studies concerning nylon 6,6 and polypropylene as thermoplastic matrices [5–8]. In this work the application of the method is extended to the study of PEEK reinforced with glass (PEEK/GF) and carbon fibres (PEEK/CF). For this purpose their stress–strain curves and fibre length distributions have been determined to calculate the interfacial shear stress. SEM observations have been carried out to verify the differences in interfacial shear stress provided by the model and to characterize the state of fibre orientation in the composites. Finally, the interest of a non-destructive ultrasonic technique for mechanical characterization of SFRTTP is evaluated by means of a comparative study of Young's modulus obtained by ultrasonic and tensile measurements.

* Author to whom correspondence should be addressed.

Present address: Laboratoire de Mécanique Physique, CNRS URA n° 867, Université de Bordeaux I, 33405 Talence, France.

2. Experimental

2.1. Materials and processing

Poly-ether-ether-ketone (PEEK) is a high temperature resistant semicrystalline thermoplastic of excellent mechanical properties and great potential as matrix material for high performance composites. The high performance of PEEK is attributed [9] to its highly aromatized ether linked chemical structure (Fig. 1).

In this work the commercial 30% by weight (W_f) short glass and carbon fibre reinforced PEEK composites—Vitrex PEEK 450 GL 30 and Vitrex PEEK 450 CA 30, respectively—were combined in appropriate proportions with unreinforced grades of the same polymer (Vitrex PEEK 450 G) to obtain the spectrum of materials with varying content of glass fibres and carbon fibres shown in Table I.

Blending was carried out in a Brabender Plasticorder PLE-650 extruder machine with a screw aspect ratio $L/D = 25$ at 400 °C. Extruded bands of 0.5 mm thickness were obtained and then pelletized by grinding. This material was then injection moulded in a Battenfield BA230 preplasticizing injection machine at varying barrel temperatures from 370 to 390 °C as the material's fibre content was increased from the unreinforced grade to the 30% fibre reinforced composites. Injection pressures and speeds were kept constant over all the range of fibre compositions and mould temperature was fixed at 165 °C. To have all materials processed in the most similar conditions even unreinforced and 30% reinforced materials were also previously extruded. At the end of the process tensile specimens (ASTM D-638) were obtained.

2.2. Microstructure characterization

2.2.1. Differential scanning calorimetry (DSC)

The calorimetric analysis was carried out with a Du Pont DSC cell equipped with a Du Pont 2000 thermal analysis system at a heating rate of 20 °C min⁻¹. Crystallinity degree of PEEK in the composites was calculated as follows

$$X_c = \frac{Q_m}{\Delta W Q_c} 100 \quad (1)$$

In this equation X_c is the degree of crystallinity of PEEK in percentage, Q_m is the melting enthalpy obtained in the DSC scan, ΔW is the weight content of PEEK in the composite, and, $Q_c = 130 \text{ J g}^{-1}$ is the melting enthalpy for fully crystallized PEEK [10].

2.2.2. Optical microscopy

A fibre suspension was prepared with washed and filtered fibres in a diluted poly(methylmethacrylate) solution in chloroform after dissolving the matrix in concentrated sulphuric acid. A microscope slide was filled with this suspension. Then the solvent was evaporated and a good dispersion of fibres in a transparent polymer film was obtained. Fibre images were taken from a Leitz Aristomet optical microscope, recorded in a Sony magnetoscope and then analysed by a commercial image analysis software (Samba 20005). Measurements were carried out counting at least 500 fibres for each sample. Finally a statistical software was used to obtain fibre length distribution histograms.

2.2.3. Scanning electron microscopy SEM

Fracture surfaces of tensile tested specimens were observed in a scanning electron microscope (SEM) Hitachi S-2700 at 15 kV. Samples were previously gold-coated to avoid electrical charges in a SC 500 sputter coater.

2.3. Mechanical characterization

2.3.1. Tensile tests

Tensile tests of injection moulded specimens (ASTM D-638) were conducted in an Instron 4301 universal testing machine at 5 mm min⁻¹ and 25 °C to determine their stress-strain behaviour. Young's modulus (E), yield and break stress (σ_y , σ_b), and their respective strains (ϵ_y , ϵ_b) were determined as the mean value of at least six determinations.

2.3.2. Ultrasonic tests

Shoulders of injection moulded specimens were tested by an ultrasonic immersion method at 25 °C and 5 MHz wave frequency. The technique used in this work is that employed by Hosten [11] to identify the anisotropic behaviour of composite materials. Since the tensile specimens' surfaces at their central parts were not wide enough to intercept completely the transducer beam, shoulder parts were used to carry out these measurements (Fig. 2). Determination of ultrasonic wave speeds in various planes of propagation permitted the identification of the elastic constants from which Young's moduli in the direction of melting flow (3) and two other perpendicular directions (1 and 2) were obtained.

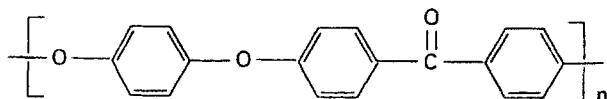


Figure 1 Chemical structure of PEEK.

TABLE I Injection moulded PEEK based materials

Fibre weight content Code	W_f (%)	Fibre volume content V_f (%)	Type of reinforcement
PEEK	0	0	unreinforced
GPEEK 10	10	5.4	glass fibres
GPEEK 20	20	11.3	glass fibres
GPEEK 30	30	17.9	glass fibres
CPEEK 10	10	7.4	carbon fibres
CPEEK 20	20	15.3	carbon fibres
CPEEK 30	30	23.1	carbon fibres

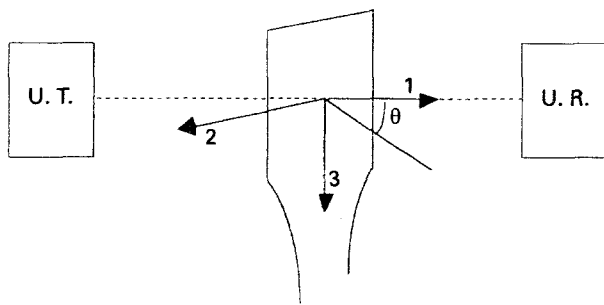


Figure 2 Injection moulding tensile specimen shoulder submitted to an ultrasonic beam at a θ angle of incidence: UT ultrasonic transmitter; UR ultrasonic receiver.

3. Results and discussion

3.1. Microstructural details

Fig. 3(a) and 3(b) show respectively the fibre length distribution histograms of 30% carbon and glass fibre reinforced composites. Similar distributions were obtained with previously extruded injection moulded composites. Average values and standard deviations calculated by means of values reported by the Gaussian decomposition curves of histograms are presented in Table II.

As can be observed lower fibre length reductions are obtained in PEEK/GF than in PEEK/CF composites. This is attributed to the higher susceptibility of carbon fibres to get attributed during processing. Moreover, composites reinforced with low contents preserve better fibres from degradation that shows the importance of fibre-fibre interactions during the breaking process of fibres.

Concerning matrix ability to crystallize, DSC experiments (see Fig. 4) did not show important variations between unreinforced PEEK and its composites. Both pure and reinforced PEEK did not present the reported [12] exothermic recrystallization peak appearing at 170°C during the scan. This is attributed to the high mould temperatures chosen during injection moulding which produces a high crystallinity degree in the matrix, reducing in this way the ability of PEEK composites to crystallize during the heating scan. The melting enthalpy of PEEK follows a linear drop with fibre content. However, as can be seen in Table III, regardless of the fibre type and content the crystallinity degree of PEEK matrix has a value of approximately 30% in both unreinforced and reinforced materials. These results would indicate that at this mould temperature neither glass nor carbon fibres induce basic changes in crystallinity degree of PEEK. In another paper we observe that at lower crystallinity values of the matrix this passive role of fibres may be modified to perform the role of nucleating sites of crystallites [13].

Traditionally in injection moulded composites, mould geometry has been considered to be the most important parameter to set up the orientation state of the fibres. Though several dimensions and gates have been considered, the most studied case has been that of edge-gated rectangular moulds. In these studies, carried out with 2.3–6 mm depth rectangular moulds [14–17], three layer structures were observed: an

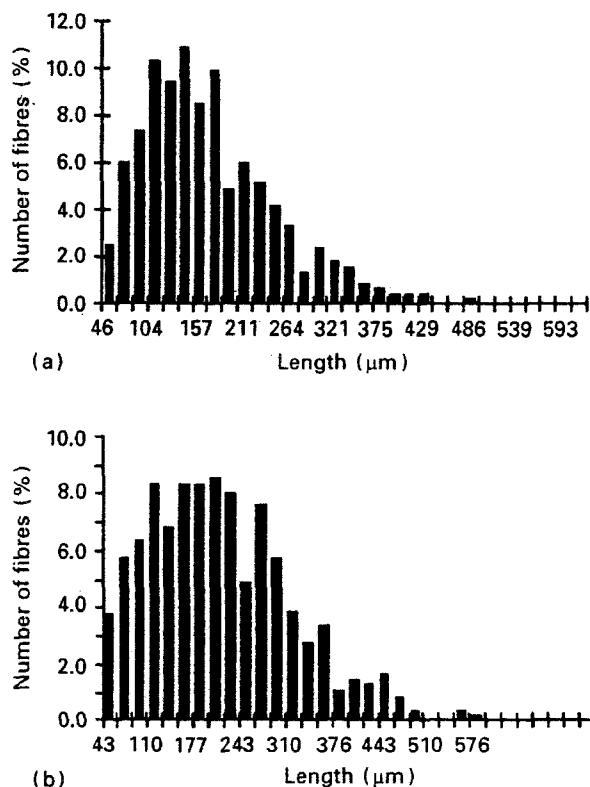


Figure 3 Fibre length distribution histograms of row composites, (a) Victrex PEEK CA 30; (b) Victrex PEEK GL 30.

TABLE II Average fibre length (L_n) and standard deviations of gaussian fibre length distributions

Material	Average fibre length(μm)	Standard deviation
GPEEK 30 (granules)	209	108
CPEEK 30 (granules)	170	93
GPEEK 30 (moulded part)	176	73
CPEEK 30 (moulded part)	103	53
GPEEK 10 (moulded part)	189	79
CPEEK 10 (moulded part)	135	87

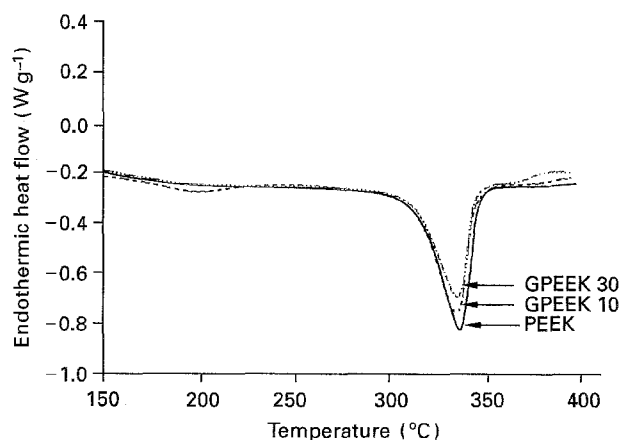


Figure 4 DSC scans at $20^{\circ}\text{C min}^{-1}$ of unreinforced PEEK and its glass fibre composites.

TABLE III Thermal properties in the nonreinforced and reinforced PEEK samples

Thermal properties	Pure	Reinforced Carbon fibres (CF)			Glass fibres (GF)		
		+ 10%	+ 20%	+ 30%	+ 10%	+ 20%	+ 30%
Melting temperature (°C)	331.2	329.6	326.9	326.0	329.5	329.4	329.5
Melting enthalpy (J g ⁻¹)	34.0	31.4	27.7	26.1	31.1	28.0	24.5
Crystallinity degree (%)	29	30	30	32	29	30	30

upper and a lower skin layer revealed fibre alignment along the melt flow direction whereas in the core they were transversely oriented. With more complicated geometries such as discs [18–19] or dogbone tensile bars [20] this type of configuration was also confirmed. In other cases different numbers of layers were observed [21–22]. The layered structures were obtained with different thermoplastics of different fibre contents processed in different conditions that demonstrates that the restrictions imposed to melt flow by the mould must be more important than the intrinsic rheological aspects of the polymeric melt. Nevertheless, this fact does not mean that material variables and injection conditions do not play any role in the constitution of layered structures. It has been demonstrated that the size of each layer and the local fibre orientation in the layer could be modified by varying the polymer matrix [23] and the injection parameters [24], that in some cases could produce the disappearance of the core. This seems to be the case for short fibre PET composites where layered structures were rarely observed [25].

SEM studies carried out with GPEEK 30 are shown in Figs 5–7. At low magnifications three distinct layers were observed in the thickness direction. Fig. 5 and Fig. 7 show the morphology of GPEEK 30 in the upper and lower skin layers respectively where most of the fibres are aligned in the melt flow direction as expected from convergent flows implicated in the central parts of injection specimens where measurements have been carried out [26–28]. Fig. 6 shows the core region of this composite in which, despite showing on average a high fibre alignment, more fibres than in the case of skin regions are observed to lie perpendicularly to the melt flow direction.

3.2. Tensile behaviour

3.2.1. Stress–strain curves

Figs 8 and 9 show respectively the stress–strain behaviour of PEEK/GF and PEEK/CF composites. The behaviour of pure PEEK is also presented. PEEK's stress shows a linear trend at low strains that is followed by a non-linear behaviour before reaching the yield point; then the stress drops to a given value which is maintained constant up to when the break is produced. The evolution of stress described here is basically that observed in semicrystalline ductile polymers [29]. Only the habitual hardening process occurring after necking is not observed in this case because fracture, led by the high crystallinity value of the matrix, occurs at low strains. This hardening process

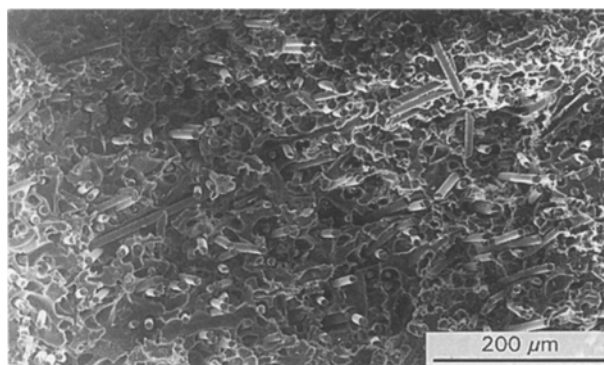


Figure 5 Fracture surface of GPEEK 30 (upper skin region).

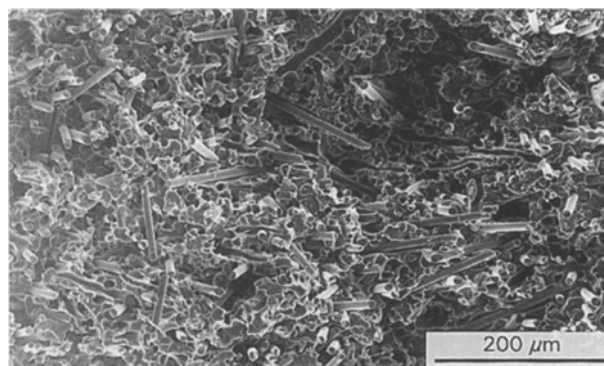


Figure 6 Fracture surface of GPEEK 30 (core region).

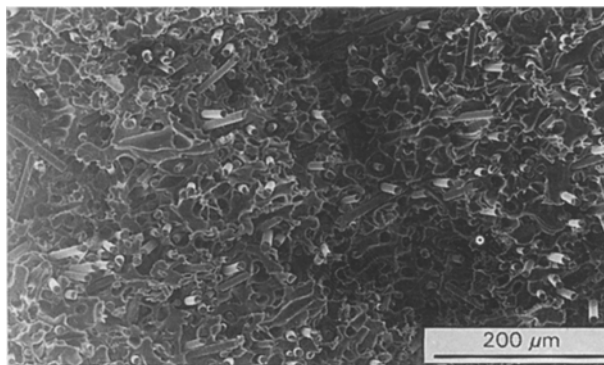


Figure 7 Fracture surface of GPEEK 30 (lower skin region).

has been observed when lower moulding temperatures were used in the manufacturing process [30].

Concerning PEEK short fibre composites, the general tendencies expected when reinforcing polymers are confirmed for both glass and carbon reinforced systems: stress–strain curves become higher and shorter as the fibre content is increased. Thus stiffness

and strength of the material are improved at the expense of the ductility.

The typical mechanical properties with their standard deviations are presented in Table IV. To the already reported [31] linear increase of Young's modulus with fibre volume content, must be added the similar behaviour found with strength in both carbon and glass fibre reinforced composite systems. Strain at break drops drastically when fibres are incorporated into the matrix. This is the reason the yield point is only observed if matrix is unreinforced or reinforced by a low content of fibres (GPEEK 10, CPEEK 10).

3.2.2. Critical fibre length and interfacial shear stress

The stress-strain values reported above were used together with the fibre length distributions to calculate

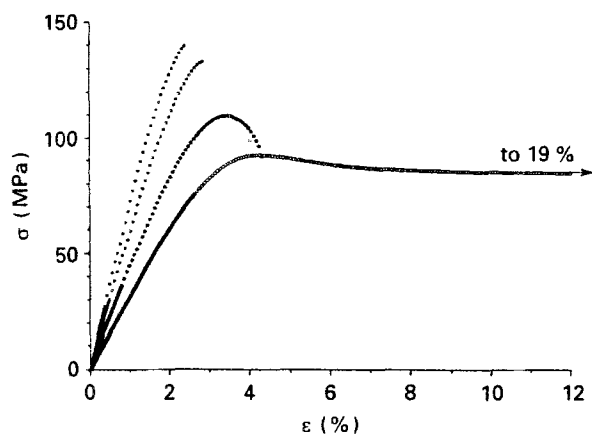


Figure 8 Stress-strain behaviour of PEEK/GF composites: (○) PEEK, (●) GPEEK 10, (□) GPEEK 20, (■) GPEEK 30.

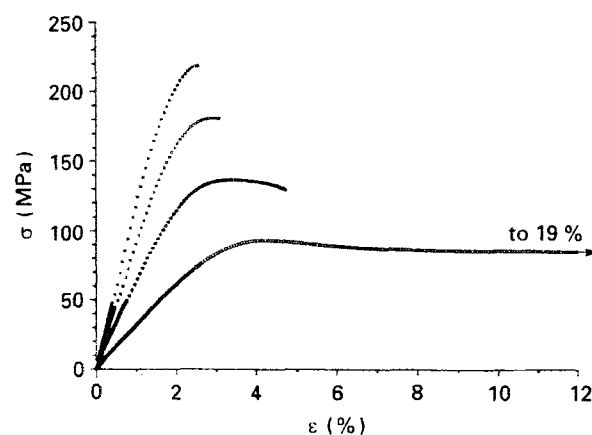


Figure 9 Stress-strain behaviour of PEEK/CF composites: (○) PEEK, (●) CPEEK 10, (□) CPEEK 20, (■) CPEEK 30.

TABLE IV Mechanical properties of PEEK/GF and PEEK/CF composites

Material	$E(\text{GPa})$	$\sigma_y(\text{MPa})$	$\epsilon_y(\%)$	$\sigma_b(\text{MPa})$	$\epsilon_b(\%)$
PEEK	3.10 ± 0.04	91.4 ± 0.6	4.1 ± 0.1	85.6 ± 3.7	19.3 ± 7.6
GPEEK 10	4.70 ± 0.42	108.9 ± 0.8	3.3 ± 0.1	98.6 ± 9.0	3.9 ± 0.5
GPEEK 20	5.98 ± 0.82	—	—	128.7 ± 3.1	2.7 ± 0.1
GPEEK 30	7.44 ± 0.35	—	—	139.0 ± 0.8	2.4 ± 0.1
CPEEK 10	6.37 ± 0.49	135.6 ± 0.6	3.4 ± 0.1	129.8 ± 1.6	4.7 ± 0.2
CPEEK 20	9.34 ± 0.52	—	—	180.4 ± 0.7	3.0 ± 0.1
CPEEK 30	12.38 ± 0.77	—	—	215.8 ± 2.1	2.5 ± 0.1

the fibre-matrix interfacial shear stress (τ) and the critical fibre length (L_c) using the model proposed by Bowyer and Bader [4].

In this theory of reinforcement the prediction of stress of a short fibre composite (σ_c) at one given strain is carried out separating the respective contributions of subcritical fibres (X), supercritical fibres (Y) and matrix (Z) which gives to the modified rule of mixtures the following form

$$\sigma_c = \eta_0(X + Y) + Z \quad (1)$$

where

$$X = \sum_{L_i < L_c} \frac{L_i \tau}{2r} V_i \quad (2)$$

$$Y = \sum_{L_j > L_c} \left(1 - \frac{\sigma_f^u r}{2L_j \tau}\right) \sigma_f^u V_j \quad (3)$$

$$Z = \sigma_m(1 - V_f) \quad (4)$$

and

$$L_c = \frac{r \sigma_f^u}{\tau}$$

Here, η_0 is the orientation efficiency factor, L the fibre length, σ_m the matrix stress at that given strain, σ_f^u the fibre ultimate stress, V_i and V_j the respective volume contents of subcritical and supercritical fibres, and r the fibres' radius.

At very low strains, when the effects of stress built up from fibre ends could be neglected, the theory gets simplified for the elastic prediction. Therefore, Young's modulus of composite is expressed as a single efficiency parameter dependent linear function of its components

$$E_c = \eta_0 E_f V_f + E_m(1 - V_f) \quad (5)$$

The theory of reinforcement presented here for short fibre reinforced composites neglects the penalty in stress contribution of fibres due to their discontinuity when fibres are longer than the strain developed during the tensile tests. Following this assumption, fibre orientation efficiency factors (η_0) have been calculated by introducing the bibliographic values of $E_{CF} = 210$ GPa and $E_{GF} = 69$ GPa, and the experimentally determined E_m , E_c and V_f values in Equation 5. After fixing the η_0 values obtained previously, critical fibre length value has been calculated for GPEEK 30 and CPEEK 30 at different strains. These calculations have been carried out trying different L_c values in Equations 1-4 until the following condition was satisfied

$$\frac{\sigma_c - \sigma_m(1 - V_f)}{X + Y} = \eta_0 \quad (6)$$

TABLE V Critical fibre length ($L_c(\mu\text{m})$) at several strains in the non-linear part of stress–strain curve

	GPEEK 30	CPEEK 30
$\varepsilon = 1.0\%$	23	31
$\varepsilon = 1.5\%$	42	47
$\varepsilon = 2.0\%$	75	82
$\varepsilon_{\text{break}}$	102	131

TABLE VI Shear stress values (τ) and the K proportionality constant at break strain for several SFRTTP

	$\tau(\text{MPa})$	K
GPEEK 30	80	0.57
CPEEK 30	202	0.93
Nylon 6,6/GF ($W_f = 30\%$) [4]	45	—
Polypropylene/GF ($W_f = 30\%$) [8]	17.6	0.19
Nylon 6,6/CF ($W_f = 30\%$) [5]	130	—

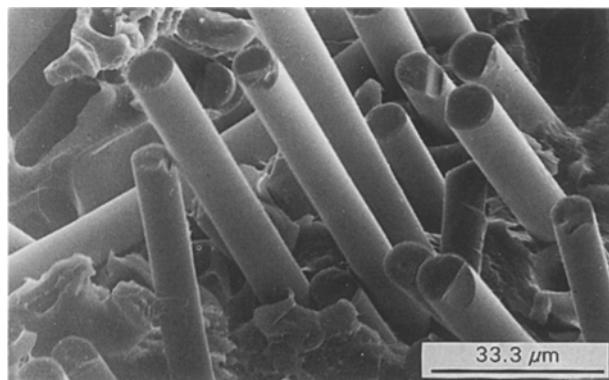


Figure 10 Scanning electron micrograph of the fracture surface of GPEEK 30.

Table V shows these results. As can be observed fibre critical length increases with strain up to strain at break for both SFRTTP composites. Moreover the L_c values are always higher for CPEEK 30 than for GPEEK 30. This is evidence – to which it should be added that given by experimentally measured shorter length values obtained in CF systems – of the higher presence of subcritical fibres in carbon fibre injection mouldings regarding GF reinforced ones.

Table VI shows the values of the shear stress at break (τ) and the proportionality constant (K) of the linear variation of τ with σ ($\tau = K\sigma$) proposed by Mittal and Gupta [6], at break strain, of these two mentioned composites together of those of similar commercial materials based in other thermoplastics [4, 5, 8]. As can be observed shear stress in CF-PEEK interface is higher than that in GF-PEEK interface. These differences are due to the higher interfacial adhesion existing in the former. SEM micrographs reveal very clean fracture surfaces in glass fibre composites (see Fig. 10) while carbon fibres are recovered by matrix at their interface (see Fig. 11). Moreover, the results show that PEEK offers to short fibre reinforced composites better interfacial properties than other thermoplastics such as polypropylene and nylon 6, 6.

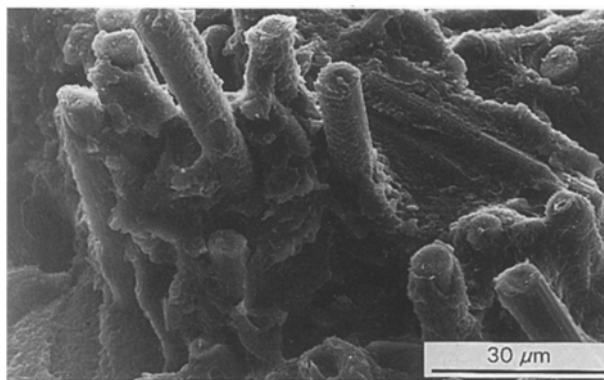


Figure 11 Scanning electron micrograph of the fracture surface of CPEEK 20.

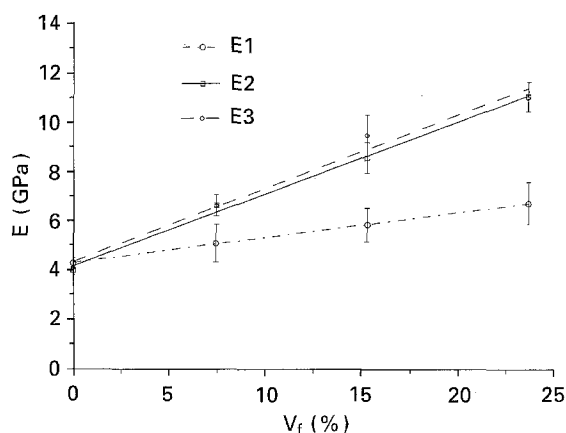


Figure 12 Ultrasonic Young's moduli of PEEK/CF in three material directions. \circ E1; \square E2; \diamond E3.

3.3. The ultrasonic Young's moduli determination

Fig. 12 shows the Young's moduli of the PEEK/CF system in the three material directions defined in Fig. 2. E_3 and E_2 , the Young's moduli in the longitudinal and transverse directions of the tensile specimen give nearly the same values at all fibre contents. The modulus in the thickness direction, E_1 , is lower. These results are interpreted as a preferential alignment of fibres in the plane 2–3. In the part of the specimen where measurements have been carried out, PEEK short fibre composites behave like quadratic composites. This type of configuration can also be inferred from similar tendencies found in PEEK/GF system.

The comparison of ultrasonic and tensile results is not an easy task. Since different geometries acting during the melt filling process are implicated, the state of orientation of fibres in central parts of the specimens submitted to tensile test and in shoulders submitted to ultrasonic tests, must not be similar. Crowson [26] showed that a higher degree of alignment is expected in parts involved in convergent melting flow processes than in those of divergent flows. In consequence higher fibre alignment is expected in tensile than in ultrasonic tested parts.

In viscoelastic polymeric materials, their elastic response is favoured at short testing times. Due to the high frequencies involved in ultrasonic measurements. Young's moduli obtained by this method are usually

TABLE VII Young's modulus in the mould filling direction by tensile (E_{3t}) and ultrasonic (E_{3u}) tests

	E_{3t} (GPa)	E_{3u} (GPa)
PEEK	3.10 ± 0.04	4.11 ± 0.47
GPEEK 10	4.70 ± 0.42	5.45 ± 0.59
GPEEK 20	5.98 ± 0.82	6.71 ± 1.27
GPEEK 30	7.44 ± 0.35	8.11 ± 1.37
CPEEK 10	6.37 ± 0.49	6.62 ± 1.3
CPEEK 20	9.34 ± 0.52	9.50 ± 0.83
CPEEK 30	12.38 ± 0.77	11.02 ± 0.66

higher than those obtained by tensile tests. PEEK matrix results (see Table VII) confirm this fact, being the ultrasonic value 31% higher than its corresponding tensile value. The comparison of results in composites should reflect these considerations.

Comparing Young's moduli of composites in the mould filling direction by ultrasonic and tensile measurements, higher E_3 values are generally found both in carbon and glass reinforced systems by ultrasonic results (CPEEK 30 is the only one giving a higher modulus by tensile). Quantitatively, however, the differences obtained in the case of composites are not as high as those found in the matrix. This could be a demonstration of the higher orientation of fibres in tensile parts than in ultrasonic parts. Moreover the $E(\text{ultrasonic})/E(\text{tensile})$ ratio is higher for PEEK/GF than in PEEK/CF systems at all fibre contents. At this point, several remarks could be made. First, the fibre volume content is higher in PEEK/CF systems. Second, these results might be interpreted as higher alignment of CF than GF in PEEK melting convergent flows, or higher alignment of the later in divergent flows or as a combination of both effects at the same time. Finally, the $E(\text{ultrasonic})/E(\text{tensile})$ ratio decreases with increasing fibre content in both composite systems as expected from the lower content of the viscoelastic component in the composite.

4. Conclusions

Microstructure studies of injection moulded short fibre PEEK samples were carried out following the evidences provided by SEM, optical microscopy and DSC experimental techniques. A layered structure with high alignment of fibres along the melt flow direction could be observed in injection moulded samples 2 mm thick submitted during processing to a convergent melting flow from examination of their fracture surfaces. Moreover, fibre length and matrix crystallinity values were determined. The former evidenced that carbon fibres were more susceptible than glass fibres to get attrited during the manufacturing process. The latter showed no effect of fibres in matrix crystallinity degree calculated from calorimetric results, whose value is reported to be approximately constant ($X_c = \sim 30\%$).

The mechanical behaviour was determined by tensile and ultrasonic tests. The use of actual tensile stress-strain curves in the Bowyer-Bader model provided higher fibre-matrix shear strength and higher

critical length values of PEEK/CF over those of PEEK/GF composites. These predictions were confirmed by SEM showing the carbon fibres had a much higher adhesion to PEEK matrix than the glass fibres. In the context offered by the theory of reinforcement above presented it was interpreted that PEEK offers better interfacial properties to fibres than other thermoplastics.

The interest of a non-destructive ultrasonic technique for mechanical characterization of SF RTP was finally evaluated comparing the Young's modulus of composites obtained by ultrasonic and tensile measurements. If effects such as the viscoelastic nature of the matrix, and the complex processing-microstructure relationships of SF RTP were considered, the tensile and ultrasonic results are seen to be compatible.

Acknowledgements

The authors thank Dr J. J. Peña for his aid in SEM. This work has been made possible by the financial support of the Spanish Ministerio de Educación y Ciencia.

References

1. "Engineering materials handbook Vol. 1. Composites", ASM International Edition, Metals Park, Ohio (1987).
2. H. L. COX, *Brit. J. Appl. Phys.* **3** (1952) 72.
3. A. KELLY and W. R. TYSON, *J. Mech. Phys. Solids* **13** (1965) 329.
4. W. H. BOWYER and M. G. BADER, *J. Mater. Sci.* **7** (1972) 1315.
5. P. T. CURTIS, M. G. BADER and J. E. BAILEY, *ibid.* **13** (1978) 377.
6. R. K. MITTAL and V. B. GUPTA, *ibid.* **17** (1982) 3179.
7. R. K. MITTAL, V. P. GUPTA and P. J. SHARMA, *ibid.* **22** (1987) 1949.
8. V. P. GUPTA, R. K. MITTAL, P. K. SHARMA, G. MEN-NIG and J. WOLTERS, *Polym. Compos.* **10** (1989) 16.
9. D. P. JONES, D. C. LEACH and D. R. MOORE, *Polymer* **26** (1985) 1385.
10. D. J. BLUNDELL and B. N. OSBORN, *ibid.* **24** (1983) 1953.
11. B. HOSTEN, *Ultrasonics* **30** (1992) 365.
12. J. KARGER-COCSIS and K. FRIEDRICH, *Plast. Rubb. Process. Appl.* **8** (1987) 91.
13. J. R. SARASUA, P. M. REMIRO and J. POUYET, in press.
14. P. SINGH and M. R. KAMAL, *Polym. Compos.* **10** (1989) 344.
15. M. J. FOLKES and D. A. M. RUSSELL, *Polymer* **21** (1980) 1252.
16. P. A. O'CONNELL and R. A. DUCKETT, *Compos. Sci. Tech.* **42** (1991) 329.
17. J. C. MALZAHN and J. M. SCHULTZ, *ibid.* **25** (1986) 187.
18. M. VINCENT and J. F. AGASSANT, *Polym. Compos.* **7** (1986) 76.
19. M. AKAY in "Interrelation between processing, structure and properties of polymeric materials", edited by J. C. Seferis and P. S. Theocaris (Elsevier Science Publishers, Amsterdam, 1984) p. 669.
20. M. BOZARTH, J. W. GILLESPIE and R. L. MCCULLOUGH, *Polym. Compos.* **8** (1987) 74.
21. M. AKAY and D. BARKLEY, *J. Mater. Sci.* **26** (1991) 2731.
22. S. KENIG, *Polym. Compos.* **7** (1986) 50.
23. P. F. BRIGHT and M. W. DARLINGTON, *Plat. Rubb. Process. Appl.* **1** (1981) 139.
24. R. BAYLEY and B. RZEPKA, *Int. Polym. Process.* **6** (1991) 35.
25. K. TAKAHASHI and N. S. CHOI, *J. Mater. Sci.* **26** (1991) 4648.
26. R. J. CROWSON, M. J. FOLKES and P. F. BRIGHT, *Polym. Engng. Sci.* **20** (1980) 925.
27. R. J. CROWSON and M. J. FOLKES, *ibid.* **20** (1980) 934.

28. R. J. CROWSON, M. J. FOLKES and D. W. SAUNDERS *ibid.* **21** (1981) 748.
29. L. E. NIELSEN "Mechanical properties of polymers and composites" Vol. 2, (Marcel Dekker Inc., New York, 1974), Chapter 5.
30. J. R. SARASUA, P. M. REMIRO and J. POUYET, in International Meeting on Composite Materials, "Advancing with Composites 1994", Milan 1994, Vol. 1, p. 437.
31. J. R. SARASUA, B. HOSTEN and J. POUYET in Proceedings of the Ninth International Congress of Composite Materials (ICCM-9), Madrid 1993, Vol. 2, p. 235

*Received 15 December 1993
and accepted 14 November 1994*